Available online at www.sciencedirect.com
SCIENCE DIRECT
Tetrahedron 62 (2006) 7014–7020
Tetrahedron

Theoretical study of the regioselectivity of the cycloaddition reaction between cyclopentadiene and methyleneketene

Yinghong Sheng and Jerzy Leszczynski*

The Computational Center for Molecular Structure and Interactions, Department of Chemistry, Jackson State University, PO Box 17910, 1400 J. R. Lynch Street, Jackson, MS 39217, USA

Received 9 January 2006; revised 13 April 2006; accepted 21 April 2006
Available online 22 May 2006

Abstract—Three possible reaction schemes for the cycloaddition reaction between methyleneketene and cyclopentadiene were studied by DFT (density functional theory) and ab initio calculations. All of these cycloaddition reactions are exothermic, concerted but nonsynchronous processes. The computed activation energies indicate that the norbornene product yielded from a 1,2-addition of methyleneketene with cyclopentadiene (reaction (1)) is the primary product. The performance of various computational methodologies, MP2, MP4, and CCSD(T), in conjunction with a wide array of basis sets, 6-31G(d), 6-311+G(d,p), aug-cc-pVDZ, and aug-cc-pVTZ, in obtaining reliable activation and reaction energies of the reactions under investigation has been critically analyzed.

1. Introduction

Heterocumulenes are highly versatile synthetic intermediates, and unlike most unsaturated compounds, they undergo either thermal [2+2] or [2+4] cycloadditions readily. This notion generates a great interest in the industrial[1] and pharmaceutical applications.[2,3] A special class of heterocumulenes, based on parent methyleneketene ($H_2C{=}C{=}C{=}O$) and its substituted derivatives, might exhibit different reaction preferences than the other previously studied ketenes.[4,5] It is known that ketenes react with cyclopentadiene in a [2+2] process forming cyclobutanones (the Staudinger reaction) rather than in a [4+2] reaction leading to norbornenones.[6–9] So far based on the studied cycloaddition of methyleneketene one assumes that their behavior is analogous to that of ketene.[10] However, a single example of the parent methyleneketene undergoing a [4+2] cycloaddition had been reported, and the only cycloaddition product, which takes place on the interior C=C double bond of methyleneketene with 5-methylene-1,3-dioxan-4,6-dione, had been experimentally and theoretically studied.[11]

The possibility of another [4+2] cycloaddition for methyleneketene, i.e., the reaction between methyleneketene and cyclopentadiene, was revealed during our research devoted to the study of the cycloaddition of cumulene.[11b,12] The cycloaddition between methyleneketene and cyclopentadiene is expected to yield a norbornene product, rather than norbornanone or 5-oxobicyclo[2.2.1]hept-2-ene. In spite of the synthetic interest in these products,[13] no theoretical study regarding this reaction has been reported. Therefore the mechanisms of these types of reactions require detailed investigation. In this paper, the possible reaction mechanisms of the [4+2] cycloaddition between methyleneketene and cyclopentadiene were theoretically studied in the gas phase and polar solvents by means of ab initio methods and density functional theory.

Due to its specific structure, methyleneketene provides three double bonds on which three possible [4+2] reactions with cyclopentadiene may take place (Scheme 1), i.e., cycloaddition with cyclopentadiene may involve either the C=C or the C=O bonds of methyleneketene: addition to the C=C double bond to give either norbornene derivative **1**

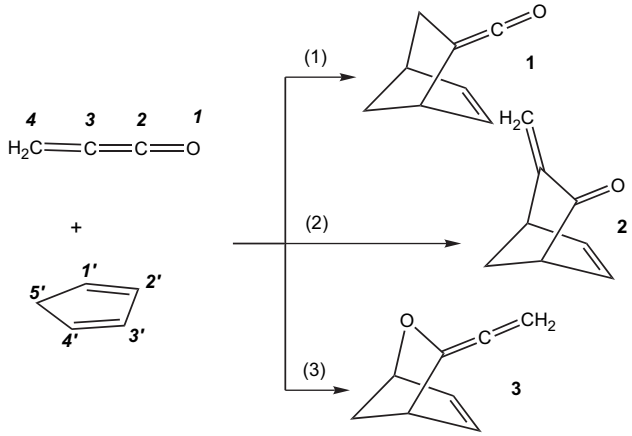

Scheme 1.

* Corresponding author. Tel.: +1 601 979 3482; fax: +1 601 979 7823; e-mail: jerzy@ccmsi.us

0040–4020/$ - see front matter © 2006 Elsevier Ltd. All rights reserved.
doi:10.1016/j.tet.2006.04.067

(bicyclo[2.2.1]hept-5-en-2-ylidene-methanone) or norbornanone derivative **2** (3-methylene-bicyclo[2.2.1]hept-5-en-2-one), or less likely addition to the C═O double bond to give 5-oxobicyclo[2.2.1]hept-2-ene derivative **3** (3-vinylidene-2-oxa-bicyclo[2.2.1]hept-5-ene).[14–16] All these possible products may have potential industrial and pharmaceutical applications.[2,17] Thus, the investigation of the regioselectivity of cycloaddition between methyleneketene and cyclopentadiene is of great interest.

2. Computational method

The geometry of the reactants, products, and transition states were optimized at the B3LYP level of theory using the 6-31G(d) basis set by means of the Berny approach, a modified Schlegel method.[18] Harmonic vibration frequency calculations were performed to confirm whether the obtained geometry represents a transition or minimum energy structure.

Inclusion of the correlation energy is necessary for a reasonable prediction of the activation energy because these contributions are often larger for the transition structures than for the minimum energy structures. In this study the energies were evaluated at the MP2/6-31G(d) level of theory using the B3LYP/6-31G(d) optimized structures. The geometry of the reactants, products, and transition states were also re-optimized at the MP2/6-31G(d) level. Entropies and enthalpies of activation were obtained at the B3LYP/6-31G(d) and MP2/6-31G(d) levels.

To better account for the effects of electron correlation, the activation and reaction energies were also evaluated at MP4, CCSD, and CCSD(T) using the geometries optimized at the MP2/6-31G(d) level.

The 6-31G(d) basis set was used for the geometrical optimization. To assess the basis set effect on the activation and reaction energies, a wide array of basis sets, namely, 6-31G(d), 6-311+G(d,p), aug-cc-pVDZ, and aug-cc-pVTZ, was used at the B3LYP and MP2 levels of theory.

The reaction and activation energies in the solvents were also evaluated at the B3LYP/6-31G(d) level by the polarized continuum model applying the integral equation formalism[19] using the geometries optimized in the gas phase. In this model, the liquid is represented by a dielectric continuum, characterized by its dielectric constant ε. The solute is placed in a cavity created in the continuum. The dielectric constants of ε=8.93 and 20.7 (that correspond to dichloromethane and acetone) were used. The specific interactions, such as hydrogen bonding are not covered by this model.

All calculations were performed using GAUSSIAN03.[20]

3. Results and discussion

3.1. Reactants and products

The qualitative picture obtained from the valence-bond diagrams and the quantitative information from the molecular orbital calculations can provide guidance for the interpretation of the behavior of methyleneketene. One of the first studies of such species were performed by Radom who calculated the π-electron distributions perpendicular to the molecular plane for the various atoms in methyleneketene using ab initio molecular orbital theory.[21]

It is well-known that methyleneketene is not linear, unlike the cumulene $H_2C{=}C{=}C{=}CH_2$. The B3LYP/6-31G(d)- and MP2/6-31G(d)-optimized geometrical parameters as well as the experimental data obtained from the microwave spectra of several isotopic species of methyleneketene[22] are shown in Figure 1. One can see that the geometrical parameters predicted at the B3LYP/6-31G(d) level are in excellent agreement with the previous microwave measurement and theoretical studies.[23] Interestingly, the B3LYP/6-31G(d) parameters are in better agreement with the experiments than those obtained from the MP2 level calculations.

The structures of three products of the Diels–Alder reaction between methyleneketene and cyclopentadiene are depicted in Figure 1. The reaction energies at the different levels of theory are summarized in Table 1. All of the reactions are exothermic. The reaction energies at the B3LYP/6-31G(d) level amount to 35.1 and 42.0 kcal/mol for reactions (1) and (2), respectively. The reaction energy for reaction (3) at the B3LYP/6-31G(d) level is predicted to be 7.7 kcal/mol; this suggests that the addition to the C═O double bond is very unfavorable compared to the additions to the C═C double bonds of methyleneketene.

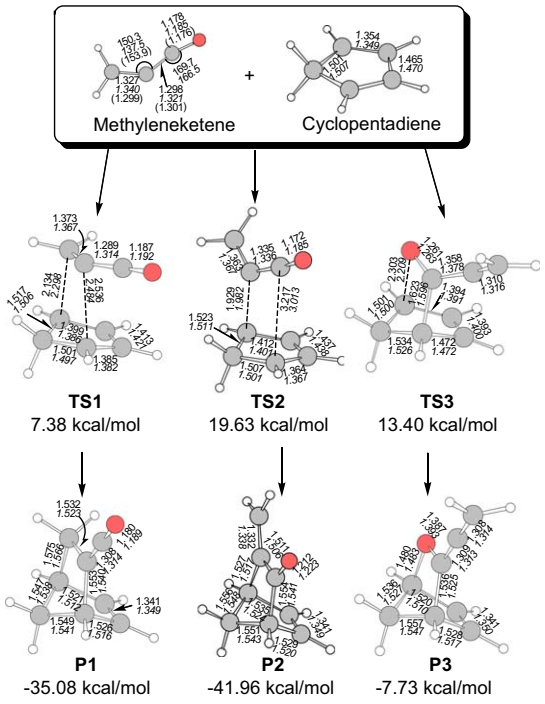

Figure 1. The B3LYP/6-31G(d)-optimized geometrical parameters for the reactants, transition structures, and products. For comparison, the MP2/6-31G(d)-optimized geometrical parameters are listed in italic. The experimental determined geometrical parameters for methyleneketene are shown in the parenthesis. The relative energies were obtained at the B3LYP/6-31G(d) level.

Table 1. The activation and reaction energies at the different levels of theory for the stationary points located on the [4+2] cycloaddition between methyleneketene and cyclopentadiene

	B3LYP[a]		MP2[b]		MP4(SDTQ)[c]	CCSD[c]	CCSD(T)[c]
	$\Delta E(\Delta E_0)/\Delta E(\Delta E_0)$	ΔH	$\Delta E(\Delta E_0)$	ΔH	ΔE	ΔE	ΔE
TS1	7.38(9.8)/*−2.21(0.2)*	8.8	−2.39(−0.2)	−1.1	2.99	10.26	6.34
TS2	19.63(20.9)/*12.89(14.1)*	20.2	12.92(13.9)	13.3	16.35	24.57	19.45
TS3	13.40(16.0)/*10.24(12.8)*	14.6	9.36(12.1)	10.7	10.44	16.35	11.70
P1	−35.08(−29.4)/*−50.08(−44.4)*	−31.1	−49.71(−43.8)	−45.4	−44.61	−45.66	−43.77
P2	−41.96(−36.6)/*−55.92(−50.6)*	−38.3	−55.51(−50.2)	−51.8	−51.14	−54.11	−51.98
P3	−7.73(−2.9)/*−15.73(−10.9)*	−4.5	−15.23(−10.4)	−11.9	−11.88	−16.35	−14.32

The energies are in kcal/mol.
[a] B3LYP/6-31G(d) energy at the B3LYP/6-31G(d) optimized structure. MP2/6-31G(d)//B3LYP/6-31G(d) energy is in italic, the zero-energy corrected energy are in the parenthesis.
[b] MP2/6-31G(d) energy at the MP2/6-31G(d) optimized structure.
[c] Single point energy using 6-31G(d) basis set at the MP2/6-31G(d) optimized structure.

The reaction energies predicted at the MP2, MP4(SDTQ), and CCSD(T) levels of theory are also listed in Table 1. From Table 1, one can see that the reaction energies at the MP2, MP4(SDTQ), and CCSD levels of theory are larger than the CCSD(T) results.

Compared to the CCSD(T) results, B3LYP underestimates the reaction energies. The differences amount to 8.7, 10.0, and 6.6 kcal/mol for reactions (1), (2), and (3), respectively. On the contrary, MP2 and CCSD overestimate the reaction energies by about 2–6 kcal/mol. The substantial differences in reaction energies between the MP2, CCSD, and the CCSD(T) values indicate that the triple substitution makes a measurable contribution to accurate description of the reaction energy.

The MP4-predicted reaction energies are in most cases in agreement with the CCSD(T) reaction energies, and the differences are smaller than 1 kcal/mol, except for the reaction energy for the C═O addition, which differs by 2.4 kcal/mol. These differences can be related to the high-order electron correlation contributions. The reason that MP4 is in the closest agreement with CCSD(T) is due to the close connection between the two methods. The SDQ components of MP4 approximate those of CCSD, while the triple components of MP4 are similar in structure to the CCSD(T) correction. Therefore, MP4 level calculations with single, double, triple, and quadruple substitutions are expected to provide reliable reaction energies.

The reaction energies were also evaluated at the MP2 level using different basis sets. As one can see from Table 2, at the MP2/6-31G(d) level, the reaction energies for the 2,3-C═C, 1,2-C═C, and C═O addition reactions are −49.7, −55.5, and −15.2 kcal/mol, respectively. The further expansion of the basis set to 6-311+G(d,p), and aug-cc-pVTZ has less impact on the accuracy of the reaction energies. The differences in the reaction energies are around 1 kcal/mol when the basis set changes from 6-31G(d) to aug-cc-pVTZ. All data are in good agreement with the CCSD(T) method.

However, the values of reaction energy were significantly affected by the size of the basis set at the B3LYP level. The differences in the reaction energies amount up to 4 kcal/mol at the B3LYP/6-31G(d) level when different basis sets were used. This indicates that B3LYP, unlike the MP2 method, is inadequate for quantitatively describing the reaction energies.

3.2. Transition states

The geometries of three transition states were first optimized at the B3LYP/6-31G(d) level, followed by the MP2/6-31G(d) single point energy evaluation. The activation energies for reactions (1), (2), and (3) are listed in Table 1. There are big differences in the activation energies between the two levels of theory. For instance, the MP2/6-31G(d)-computed activation energy for TS1 is −2.2 kcal/mol, while the B3LYP/6-31G(d)-predicted activation energy is 7.4 kcal/mol. The difference amounts to 9.5 kcal/mol!

Since the different activation values are predicted by B3LYP/6-31G(d) and MP2/6-31G(d) calculations, it is necessary to benchmark the study of the reaction under investigation in order to find a reliable approach to predict the reaction

Table 2. The basis set effect on the activation and reaction energies at the B3LYP and MP2 levels of theory

	B3LYP[a]				MP2[b]			
	6-31G(d)	6-311+G(d,p)	Aug-cc-pVDZ	Aug-cc-pVTZ	6-31G(d)	6-311+G(d,p)	Aug-cc-pVDZ	Aug-cc-pVTZ
TS1	7.4	10.0	8.4	10.9	−2.4	−4.6	−9.1	−7.4
TS2	19.6	22.4	20.2	23.1	12.9	10.5	6.9	9.1
TS3	13.4	17.9	14.3	18.5	9.4	9.9	4.7	6.8
P1	−35.1	−29.5	−32.7	−27.8	−49.7	−49.3	−51.0	−49.3
P2	−42.0	−35.6	−39.5	−34.1	−55.5	−54.1	−57.0	−54.6
P3	−7.7	−1.2	−5.0	−1.0	−15.2	−13.3	−16.5	−16.3

The energies are in kcal/mol.
[a] At the B3LYP/6-31G(d) optimized structure.
[b] At the MP2/6-31G(d) optimized structure.

activation barriers and the structural and electronic features of these kinds of reactions.

3.2.1. Consideration of electron correlation. It is well known that the Hartree–Fock-based methods significantly overestimate the energy barrier, and increasing the basis set quality even worsens the results.[24] In order to obtain the correct energetics, it is very important to include dynamic correlation. Therefore the single point energies at the MP4, CCSD, and CCSD(T) levels using the MP2/6-31G(d) optimized structures were computed and listed in Table 1. The T1 diagnostic values[25] for the transition structures were also calculated at the CCSD level, and small values (<0.018) T1 diagnostic indicates that the coupled cluster method provides reliable estimate of the reaction barrier height.

B3LYP and MP2 take into account the electron correlation in quite different ways. Comparing with the CCSD(T) computed energies, MP2 underestimates the activation barrier for reactions (1) and (2) by about 8.7 and 6.6 kcal/mol, respectively. Thus MP2 is clearly unsuitable for quantitative prediction. This is in agreement with a recent study of regioselectivity, stereoselectivity, and asynchronicity in a series of hetero-Diels–Alder reactions.[26] When full MP4 method with single, double, triple, and quadruple substitutions is considered, the activation energy is slightly improved; however, it becomes underestimated compared to the CCSD(T) results. The MP4 level activation energies are about 3.0 kcal/mol lower than the CCSD(T)-predicted results.

It is interesting to notice that the gradient-corrected hybrid density functional method, B3LYP, has shown excellent agreement with the CCSD(T) results. By comparing the activation energies listed in Table 1, the activation energies obtained at the B3LYP/6-31G(d) level differ from the CCSD(T) energies by only about 1.0, 0.2, and 1.7 kcal/mol for reactions (1), (2), and (3), respectively.

3.2.2. Basis set effect on transition structures. The 6-31G(d) basis set was used throughout for the geometry optimization of the transition states. The further expansion of the basis set has less impact on the accuracy of the molecular parameters.[27,28] Only minor changes of the geometrical parameters were observed in selected organic systems when the basis set was extended in the B3LYP calculations. The 6-31G(d) basis set is a good compromise between efficiency and accuracy.[29] We have also used the 6-311+G(d) and aug-cc-pVDZ basis sets for some of the studied species, and the geometrical parameters are essentially the same.[30] Therefore we will only discuss the geometries obtained from the 6-31G(d) basis set, unless otherwise mentioned. The transition states were also optimized using the MP2/6-31G(d) method; the geometries obtained at the B3LYP/6-31G(d) and MP2/6-31(d) levels are close to each other.

3.2.3. Basis set effect on activation energy. The activation energies computed at the B3LYP and MP2 levels using different basis sets are listed in Table 2. The results demonstrate that the activation energies at the B3LYP level had less variation as a function of the basis set than the MP2 results. B3LYP/6-31G(d) is expected to yield reliable activation energies, while the MP2 method underestimates the activation energy.

In brief, B3LYP/6-31G(d) method predicts reliable geometrical parameters for the reactants, products, and transition structures. Though the level of electron correlation is of importance for quantitative prediction of reaction and activation energies, B3LYP/6-31G(d) method can be still used for qualitative description of the energetics of the reactions under investigation. Therefore, only the B3LYP/6-31G(d) results will be used for further discussion of the reaction mechanism, unless otherwise mentioned.

3.2.4. Discussion. We started with reaction (1) between methyleneketene and cyclopentadiene, which takes place on the C3═C4 bond of methyleneketene. A transition state TS1 (see Fig. 1) was located and characterized. The main geometrical parameters of the stationary point, optimized at the B3LYP/6-31G(d) and MP2/6-31G(d) levels, are shown in Figure 1.

The distances of C4–C1′ and C3–C4′ are 2.134 and 2.536 Å, respectively, at the B3LYP/6-31G(d) level. The C4–C1′ distance obtained at the MP2/6-31G(d) level is slightly longer (2.298 Å), while the C3–C4′ distance is slightly shorter (2.484 Å). The results of both methods indicate that the reaction appears to be concerted but nonsynchronous.

Due to the attack of methyleneketene, the five carbon atoms of cyclopentadiene are no longer on the same plane, the dihedral angle C2′–C3′–C4′–C5′ amounts to −18.1° at the B3LYP/6-31G(d) level. The methyleneketene moiety is almost parallel to the cyclopentadiene moiety plane. The C2–C3–C4 angle amounts to 149.7°, slightly smaller than that in methyleneketene.

Mulliken population shows that methyleneketene donates 0.19 units of negative charge to cyclopentadiene in TS1. The activation barrier for TS1 is predicted to be 7.4 kcal/mol at the B3LYP/6-31G(d) level.

A transition state (TS2) was located and characterized for the cycloaddition reaction with cyclopentadiene taking place on C2═C3 double bond of methyleneketene. The selected geometrical parameters for the optimized transition structure at both the B3LYP/6-31G(d) and MP2/6-31G(d) levels are shown in Figure 2. Reaction (2) is also a concerted but nonsynchronous. The B3LYP/6-31G(d)-predicted C3–C1′ distance amounts to 1.929 Å, much shorter than the C2–C4′ distance (3.217 Å at the B3LYP/6-31G(d) level). Only a 0.03 e charge was transferred from methyleneketene to cyclopentadiene. The activation barrier of this reaction is 19.6 kcal/mol, much higher than reaction (1).

In addition to the two approaching modes considered earlier, the possibility of a cycloaddition reaction with cyclopentadiene taking place on the C═O bond of methyleneketene was also studied. A transition state (TS3) was located. As one can see from Figure 1, the C2–C4′ distance in the transition structure TS3 is predicted to be 1.623 Å at the B3LYP/6-31G(d) level. This indicates that the C2–C4′ bond is almost formed in transition structure TS3. The O1–C1′ bond is not yet formed; the distance between O1 and C1′ is 2.303 Å at the B3LYP/6-31G(d) level. The formation of the C2–C4′ bond in TS3 raises the question of whether reaction (3) is a step-wise reaction. Attempts have been made,

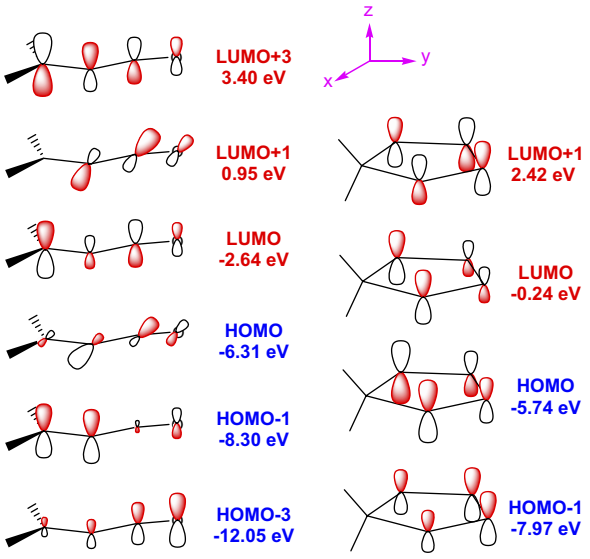

Figure 2. The energy levels of the frontier orbitals at the B3LYP/6-31G(d) level. The sizes of orbital coefficients on each atom of methyleneketene and cyclopentadiene are represented by the sizes of lobes on the orbitals.

however, no other possible transition state or intermediate on the reaction potential surface was located. Moreover, the IRC analysis shows that TS3 is directly connected with the reactants and the final [4+2] cycloaddition product. Therefore, we concluded that it is a concerted but nonsynchronous reaction. Mulliken population analysis shows that there is 0.24 e charge transfer from methyleneketene to cyclopentadiene in TS3. The activation barrier for TS3 is predicted to be 13.4 kcal/mol at the B3LYP/6-31G(d) level.

3.3. Frontier orbital analysis

FMO (frontier molecular orbital) theory has been useful in rationalizing the regioselectivity preferences of these cycloadditions. The cycloaddition can be either $HOMO_{(diene)}$–$LUMO_{(dienophile)}$ or $HOMO_{(dienophile)}$–$LUMO_{(diene)}$, depends on the direction of electron transfer during the reaction. The interaction between the frontier orbitals is expected to be stronger if the difference of the orbital energy levels is smaller and as a result the reaction will proceed easier. The greatest overlap of these orbitals occurs when the nucleophile interacts at the site of the compound that has the largest LUMO coefficient. Similarly, the electrophilic addition takes place most likely at the most nucleophilic terminus of a diene with the largest HOMO coefficient, and this terminus should become attached to the site of dienophile with the largest LUMO coefficient. Therefore, the regiochemical preference can be understood by examining the orbital coefficients on the individual atom.

By means of an analysis of the frontier molecular orbitals of the reactants (see Fig. 2) and the direction of electron transfer described in the preceding section, one can recognize that, for reaction (1), TS1 is mostly stabilized by the interaction of the HOMO-1 of methyleneketene with the LUMO of cyclopentadiene. The coefficients on C3 and C4 of methyleneketene are of approximately the same size, with the coefficient on C4 being slightly larger than that on C3; therefore, the slightly stronger orbital overlap between C4 and C1′ results in a shorter C4–C1′ distance in TS1. The energy gap of this FMO interaction amounts to 8.06 eV at the B3LYP/6-31G(d) level.

In transition state TS2, 0.03 e charge was transferred from methyleneketene to cyclopentadiene. By analyzing the frontier orbitals of the reactants shown in Figure 2, one can draw the conclusion that it is the interaction of HOMO of methyleneketene with LUMO of cyclopentadiene that stabilizes TS2. The larger orbital coefficients for the bonding atoms are localized on C3 of methyleneketene and C1′ of cyclopentadiene. This leads to a much shorter distance between the C3 and C1′ atoms than that between the C2 and C4′ atoms in TS2. The energy gap of this FMO interaction is 6.07 eV at the B3LYP/6-31G(d) level.

As for reaction (3), only the interaction of LUMO of cyclopentadiene with HOMO-3 of methyleneketene stabilizes TS3. However, this energy gap of FMO interaction is 11.08 eV at the B3LYP/6-31G(d) level, much higher than the energy gaps of the FMO interactions in TS1 and TS2. It is also known that the C═O π bond is stronger than the C═C π bond, therefore attack on the C═O bond is less probable. All these factors lead to the fact that reaction (3) has the highest energy barrier.

It is also interesting to notice that the energy gap of the FMO interaction in TS2 is lower by about 2.0 kcal/mol than that of TS1. However, TS2 possesses a higher activation barrier than TS1. The reason why TS1 is characterized by a lower activation energy can be interpreted by analyzing the orientation of the FMO interactions in TS1 and TS2. From Figure 1, one can see that the approaching modes of methyleneketene to cyclopentadiene are different in the structures TS1 and TS2. In TS1, the p_z orbital of methyleneketene interacts with the LUMO of cyclopentadiene, while the overlap between the p_x orbital of methyleneketene and the p_z orbital of cyclopentadiene stabilizes TS2. The latter approaching mode induces a strong steric repulsion between the CH_2 group of methyleneketene and cyclopentadiene in TS2 and thus destabilizes TS2. As a result, a higher activation barrier is observed. Therefore the cycloaddition at the terminal C═C bond of methyleneketene is most likely to be observed. This is different than in the case of the cycloaddition between methyleneketene and 5-methylene-1,3-dioxan-4,6-dione in which the addition takes place on the interior C═C double bond of methyleneketene.[11]

To investigate the electrostatic rationale for the intrinsic preference of the regioselectivity of addition of cyclopentadiene to methyleneketene, the solvent effects and their influence on the stabilities of transition structures were predicted with the polarized continuum model using the integral equation formalism.[19] The reference geometries optimized in the gas phase were used. In the gas phase, larger charge transfer in TS1 and TS3 than in TS2 was predicted. The values of the charge transfer are further enhanced in the polar medium, and the activation energies of TS1 and TS3 are lowered in the polar solvents. As one can see from Table 3, the activation energies for TS1 and TS3 decrease from 7.4 and 13.4 kcal/mol in the gas phase to 5.8 and 10.7 kcal/mol in dichloromethane and 5.6 and 10.4 kcal/mol in acetone,

Table 3. The B3LYP/6-31G(d) level activation energies in the gas phase and in the solutions

	Gas phase	Dichloromethane (ε=8.93)	Acetone (ε=20.7)
Reaction (1)	7.4	5.8	5.6
Reaction (2)	19.6	21.0	21.2
Reaction (3)	13.4	10.7	10.4

respectively. However, the cycloaddition taking place on the interior C═C bond of methyleneketene is hampered by a polar solvent. This suggests that a polar medium facilitates reaction (1).

4. Conclusions

The reaction mechanisms of the [4+2] cycloaddition between methyleneketene and cyclopentadiene have been investigated by ab initio and density functional theory calculations. According to the obtained results we draw the following conclusions.

(1) There are three possible reaction mechanisms for the cycloaddition between methyleneketene and cyclopentadiene, as shown in Scheme 1. The cycloadditions at different double bonds of methyleneketene are all concerted but nonsynchronous processes. An analysis based on frontier molecular orbitals shows that the reaction mechanisms correspond to the [4+2] description.
(2) All the reactions are exothermic; however, the small exothermicity of the addition to the C═O double bond suggests that reaction (3) is less favorable compared to additions to the C═C double bonds of methyleneketene (reactions (1) and (2)).
(3) The activation barriers for the cycloaddition of methyleneketene with cyclopentadiene are 7.4, 19.6, and 13.4 kcal/mol at the B3LYP/6-31G(d) level for reactions (1), (2), and (3), respectively. These computational results show that the energy barrier for the reaction leading to the 1,2-adduct norbornene (reaction (1)) is the lowest one. The predicted solvent effect indicates that reaction (1) is facilitated in a polar solvent.
(4) The performance of various computational methodologies in obtaining activation as well as reaction energies of the reactions under investigation has been critically analyzed. The hybrid density functional B3LYP method shows excellent agreement with the CCSD(T) method in obtaining activation energies, and it shows less variation as a function of basis set. On the contrary, the activation energies obtained at the MP2 level are underestimated, and thus the MP2 method is inadequate for the study of the Diels–Alder reactions. It should be noted that B3LYP, which works well for the activation energy, yet significantly underestimates the reaction energies and is sensitive to the size of basis set. For a quantitative description of the reaction energy, full MP4 level method with single, double, triple, and quadruple substitutions is necessary.

Acknowledgements

This work was supported NSF-EPSCoR Grant No.02-01-0067-08, and the Army High Performance Computing Research Center under the auspices of the Department of the Army, Army Research Laboratory cooperative agreement number DAAH04-95-2-0003/contract number DAAH04-95-C-0008. This work does not necessarily reflect the policy of the government, and no official endorsement should be inferred.

Supplementary data

The Cartesian coordinates of the optimized stationary point structures (in Å) for the cycloadditions between methyleneketene and cyclopentadiene at the B3LYP/6-31G(d) and MP2/6-31G(d) levels of theory (PDF). The geometrical parameters of optimized transition structures TS1 and TS3 at the B3LYP/6-31G(d), MP2/6-31G(d), B3LYP/6-311+G(d,p), and B3LYP/aug-cc-pVTZ levels. Supplementary data associated with this article can be found in the online version, at doi:10.1016/j.tet.2006.04.067.

References and notes

1. Abd-El-Aziz, A. S.; Edel, A. L.; May, L. J.; Epp, Karen M.; Hutton, H. M. *Can. J. Chem./Rev. Can. Chim.* **1999**, *77*, 1797.
2. Palle, V. P.; Balachandran, S.; Salman, M.; Kukreja, G.; Gupta, N.; Ray, A.; Dastidar, S. G. *PCT Int. Appl.* **2005**, 99.
3. Kraka, Elfi; Cremer, Dieter *J. Am. Chem. Soc.* **2000**, *122*, 8245.
4. Brahms, John C.; Dailey, William P. *Tetrahedron Lett.* **1990**, *31*, 1381.
5. (a) Scott, A. P.; Radom, L. *J. Mol. Struct.* **2000**, *556*, 253; (b) Park, Kyungtae; Lee, Sungyul; Lee, Yongsik. *Bull. Korean Chem. Soc.* **1999**, *20*, 809; (c) Chapman, Orville L.; Miller, Michael D.; Pitzenberger, Steven M. *J. Am. Chem. Soc.* **1987**, *109*, 6867.
6. (a) Salzner, U.; Bachrach, S. M. *J. Org. Chem.* **1996**, *61*, 237; (b) Woodward, R. B.; Hoffmann, R. *Angew. Chem., Int. Ed. Engl.* **1969**, *8*, 781.
7. Tidwell, T. T. *Ketene*; Wiley: New York, NY, 1995.
8. Wentrup, C.; Heilmeyer, W.; Kollenz, G. *Synthesis* **1994**, 1219.
9. (a) Chou, C.; Birney, D. M. *J. Am. Chem. Soc.* **2002**, *124*, 5231; (b) Seidl, E. T.; Schaefer, H. F., III. *J. Am. Chem. Soc.* **1991**, *113*, 5195; (c) Hyatt, J. A.; Raynolds, P. W. *Org. React.* **1994**, *45*, 159.
10. (a) Houk, K. N.; Li, Y.; Evanseck, J. D. *Angew. Chem., Int. Ed. Engl.* **1992**, *31*, 682; (b) Wang, X.; Houk, K. N. *J. Am. Chem. Soc.* **1990**, *112*, 1754; (c) Xu, Z. F.; Fang, D. C.; Fu, X. Y. *J. Mol. Struct. (THEOCHEM)* **1994**, *305*, 191; (d) Fang, D. C.; Fu, X. Y. *Chem. Phys. Lett.* **1996**, *259*, 265; (e) Fang, D. C.; Fu, X. Y. *Int. J. Quantum Chem.* **1996**, *57*, 1107.
11. (a) Brown, R. F. C.; Eastwood, F. W.; MeMullen, G. L. *Aust. J. Chem.* **1977**, *30*, 179; (b) Sheng, Y.-H.; Fang, D.-C.; Wu, Y.-D.; Fu, X.-Y.; Jiang, Y.-S. *J. Mol. Struct. (THEOCHEM)* **1999**, *488*, 187.
12. (a) Sheng, Y.-H.; Fang, D.-C.; Wu, Y.-D.; Fu, X.-Y.; Jiang, Y. *THEOCHEM* **1999**, *467*, 31; (b) Sheng, Y.; Leszczynski, J. In preparation.
13. (a) Jang, H.-Y.; Huddleston, R. R.; Krische, M. J. *Angew. Chem., Int. Ed.* **2003**, *42*, 4074; (b) Zimmerman, H. E.; Wang, P. *Can. J. Chem.* **2003**, *81*, 517; (c) Tanaka, K.; Watanabe, T.; Ohta, Y.; Fuji, K. *Tetrahedron Lett.* **1997**, *38*, 8943.

14. Malinovskii, M. S.; Kas'yan, L. I.; Ovsyanik, V. D. *Zh. Org. Khim.* **1973**, *9*, 2425.
15. Keeffe, J. R. *J. Phys. Org. Chem.* **2004**, *17*, 1075.
16. Carrupt, P. A.; Vogel, P. *THEOCHEM* **1985**, *25*, 9.
17. Kraka, E.; Cremer, D. *J. Am. Chem. Soc.* **2000**, *122*, 8245.
18. Schlegel, H. B. *J. Comput. Chem.* **1982**, *3*, 214.
19. Cances, M. T.; Mennucci, V.; Tomasi, J. *J. Chem. Phys.* **1997**, *107*, 3032.
20. Frisch, M. J.; Trucks, G. W.; Schlegel, H. B.; Scuseria, G. E.; Robb, M. A.; Cheeseman, J. R.; Montgomery, J. A., Jr.; Vreven, T.; Kudin, K. N.; Burant, J. C.; Millam, J. M.; Iyengar, S. S.; Tomasi, J.; Barone, V.; Mennucci, B.; Cossi, M.; Scalmani, G.; Rega, N.; Petersson, G. A.; Nakatsuji, H.; Hada, M.; Ehara, M.; Toyota, K.; Fukuda, R.; Hasegawa, J.; Ishida, M.; Nakajima, T.; Honda, Y.; Kitao, O.; Nakai, H.; Klene, M.; Li, X.; Knox, J. E.; Hratchian, H. P.; Cross, J. B.; Bakken, V.; Adamo, C.; Jaramillo, J.; Gomperts, R.; Stratmann, R. E.; Yazyev, O.; Austin, A. J.; Cammi, R.; Pomelli, C.; Ochterski, J. W.; Ayala, P. Y.; Morokuma, K.; Voth, G. A.; Salvador, P.; Dannenberg, J. J.; Zakrzewski, V. G.; Dapprich, S.; Daniels, A. D.; Strain, M. C.; Farkas, O.; Malick, D. K.; Rabuck, A. D.; Raghavachari, K.; Foresman, J. B.; Ortiz, J. V.; Cui, Q.; Baboul, A. G.; Clifford, S.; Cioslowski, J.; Stefanov, B. B.; Liu, G.; Liashenko, A.; Piskorz, P.; Komaromi, I.; Martin, R. L.; Fox, D. J.; Keith, T.; Al-Laham, M. A.; Peng, C. Y.; Nanayakkara, A.; Challacombe, M.; Gill, P. M. W.; Johnson, B.; Chen, W.; Wong, M. W.; Gonzalez, C.; Pople, J. A. *Gaussian 03, Revision C.02*; Gaussian: Wallingford, CT, 2004.
21. Radom, L. *Aust. J. Chem.* **1978**, *31*, 1.
22. (a) Brown, R. D.; Godfrey, P. D.; Champion, R.; McNaughton, D. *J. Am. Chem. Soc.* **1981**, *103*, 5711; (b) Taylor, P. R. *J. Comput. Chem.* **1984**, *5*, 589; (c) Brown, R. D.; Champion, R.; Elmes, P. S.; Godfrey, P. D. *J. Am. Chem. Soc.* **1985**, *107*, 4109.
23. (a) See Ref. 22b; (b) See Ref. 5a; (c) Brown, Ronald D.; Dittman, Ronald G. *Chem. Phys.* **1984**, *83*, 77.
24. Dinadayalane, T.; Vijaya, R.; Smitha, A.; Sastry, G. N. *J. Phys. Chem. A* **2002**, *106*, 1627.
25. Lee, T. J.; Taylor, P. R. *Int. J. Quant. Chem. Symp.* **1989**, *23*, 199.
26. Park, Y. S.; Kim, W. K.; Kim, Y. B.; Lee, I. *J. Org. Chem.* **2000**, *65*, 3997.
27. (a) Hariharan, P. C.; Pople, J. A. *Chem. Phys. Lett.* **1972**, *66*, 217; (b) Hehre, W. J.; Radom, L.; Schleyer, P. v. R.; Pople, J. A. *Ab Initio Molecular Orbital Theory*; Wiley: New York, NY, 1986; (c) Sheng, Y.; Leszczynski, J.; Garcia, A. A.; Rosario, R.; Gust, D.; Springer, J. *J. Phys. Chem. B* **2004**, *108*, 16233.
28. (a) Bauschlicher, C. W. *Chem. Phys. Lett.* **1995**, *246*, 40; (b) El-Azhary, A. A.; Suter, H. U. *J. Phys. Chem.* **1996**, *100*, 15056.
29. (a) Holmén, A.; Broo, A. *Int. J. Quantum Chem.* **1995**, *QBS22*, 113; (b) Broo, A.; Holmén, A. *Chem. Phys.* **1996**, *211*, 147.
30. See Supplementary data.